CHAPTER 8

Environmental 24-hour cycles are essential for health

Eliane A. Lucassen,[1] Claudia P. Coomans,[1] Maaike van Putten,[2] Suzanne R. de Kreij,[1] Jasper H.L.T. van Genugten,[1] Robbert P.M. Sutorius,[1] Karien E. de Rooij,[3,6] Martijn van der Velde,[3] Sanne L.Verhoeve,[1] Jan W.A. Smit,[5] Clemens W.G.M. Löwik,[3] Hermelijn H. Smits,[4] Bruno Guigas,[4,7] Annemieke M. Aartsma-Rus,[2] Johanna H. Meijer[1]

Submitted.

1. Laboratory for Neurophysiology, Department of Molecular Cellular Biology, Leiden University Medical Center, the Netherlands.
2. Department of Human Genetics, Leiden University Medical Center, the Netherlands.
3. Department of Radiology, Leiden University Medical Center, the Netherlands.
4. Department of Parasitology, Leiden University Medical Center, the Netherlands.
5. Department of Medicine, Division of Endocrinology, Radboud University Medical Center, the Netherlands.
6. Percuros BV, the Netherlands.
7. Deptartment of Molecular Cellular Biology, Leiden University Medical Center, the Netherlands.

"Secundum naturam vivere" - Seneca, Letters to Lucilius, letter 5

Abstract

Circadian rhythms are deeply rooted in the biology of virtually all organisms. The pervasive use of artificial lighting in modern society disrupts circadian rhythms and can be detrimental to our health. To investigate the relationship between disrupting circadian rhythmicity and disease, we exposed mice to continuous light (LL) for 24 weeks and measured several major health parameters. Long-term neuronal recordings revealed that 24 weeks of LL reduced rhythmicity in the central circadian pacemaker of the suprachiasmatic nuclei (SCN) by 70%. Strikingly, LL exposure also reduced skeletal muscle function (forelimb grip strength, wire-hanging duration, and grid-hanging duration), caused trabecular bone deterioration, and induced a transient pro-inflammatory state. After the mice were returned to a standard light-dark cycle, the SCN neurons rapidly recovered their normal high-amplitude rhythm, and the aforementioned health parameters returned to normal. These findings strongly suggest that a disrupted circadian rhythm reversibly induces detrimental effects on multiple biological processes.

Introduction

Virtually all organisms have measurable circadian rhythms that help them anticipate and adapt to the environmental day-night cycle. In mammals, these circadian rhythms are orchestrated by neurons within the suprachiasmatic nucleus (SCN), which is located in the anterior hypothalamus. The SCN conveys temporal information to peripheral tissue oscillators, thus producing synchronized circadian rhythms in many bodily processes, including muscle function, bone metabolism, and immune system function.[1-4] Under evolutionary pressure, the circadian system evolved as a robust mechanism for adapting to life in a cyclic environment. Thus, we hypothesize that organisms require clear external cycles in order to maintain a healthy state and that absence of external rhythmicity is detrimental for health.

The use of artificial lighting in modern society—particularly during the night—disrupts the natural robust environmental cycle and is a risk factor for frailty.[5] Nowadays, 75% of the world's population is exposed to light during the night.[6] Moreover, the prevalence of shift work is relatively high around the globe; approximately 20% of workers in Europe, 29% of Americans, and 36% of Chinese and Koreans are engaged in shift work.[7-8] Importantly, epidemiological studies of shift workers revealed increased prevalence of breast cancer,[9] metabolic syndrome,[10] osteoporosis,[11] and bone fractures[12] in this population. In addition, individuals who are exposed to more light at night tend to have decreased sleep quality,[13] increased body weight,[14] and a higher prevalence of cardiovascular disease.[15] Although these studies suggest a correlation between artificial light exposure and health, they cannot determine whether this relationship is causal. Animal studies have shown that aberrant light exposure can affect both the immune system[16-18] and metabolic function.[19-20] However, in these studies, the exposure to light was relatively brief; therefore, the results cannot be translated directly to humans, who are often chronically exposed to disruptions in circadian rhythm.

To test whether long-term exposure to an aberrant light-dark cycle affects these health parameters, and to test whether these effects are reversible, we exposed mice to continuous light (LL) for 24 weeks, followed by 24 weeks in a standard light-dark (LD) cycle. To measure rhythmicity in the central clock, we performed *in vivo* electrophysiological recordings in the SCN of freely moving mice implanted with stationary electrodes. Although short-term exposure to LL has been reported to reduce SCN rhythmicity,[21-23] whether the effects of long-term LL exposure are chronic has not been studied previously. This issue is particularly important, as the SCN is highly plastic and can adapt to changes in photoperiod, even after exposure for three weeks or longer.[24] We measured the effect of long-term LL on skeletal muscle function, bone microstructure, and immune system function at various time points during and following 24 weeks of LL exposure. Our results support the hypothesis that long-term exposure to LL conditions has significant detrimental effects on a wide range of

relevant health parameters; moreover, the majority of these parameters rapidly returned to normal upon restoring the LD cycle. Thus, our results provide compelling evidence that an absence of environmental rhythmicity plays a causal role in susceptibility to disease.

Results

Reduced behavioral rhythms in continuous light

Wild-type mice (*n* = 134) were exposed to continuous light (LL) for 24 weeks ("experimental phase"), followed by a 12h:12h light-dark (LD) cycle for 24 weeks ("recovery phase"); as a control group, a separate set of age-matched mice (*n* = 119) were exposed to an LD cycle for the entire 48 weeks (**Fig. 1**). Although the strength of the circadian rhythm decreased with age in both the LL and LD groups, this effect was significantly greater in the LL mice compared to the control mice (**Fig. 1A-B**). At 2, 8, 16, and 24 weeks, the behavioral rhythm in the mice in the LL group was 19%, 36%, 50%, and 44% smaller, respectively, compared to the control group. Two and 8 weeks after returning to the light-dark cycle, rhythm strength had increased by 79% ($P < 0.001$) and 104% ($P < 0.001$), respectively, compared to rhythm strength at 24 weeks in LL. The period of behavioral rhythm was approximately 25.5 hours in the LL group, did not change over time, and recovered to 24 hours during the recovery phase (**Fig. 1C**). Mice in the LL group had a slight but significant decrease in activity after 2 weeks in continuous light; however, activity levels did not differ significantly between the two groups at any other time point (**Fig. 1D**). Upon returning to a standard light-dark cycle, the mice in the LL group rapidly recovered in terms of both rhythm period and rhythm strength (analyzed using the moving averages method; **Fig. 1E-F**). With respect to metabolism, the mice in the LL group were significantly heavier than age-matched mice in the control group, weighing an average of 2.8 and 2.4 g more at 8 and 24 weeks, respectively. Similarly, unfasted glucose levels were generally higher in the mice in the LL group throughout of the experimental phase, and this difference reached significance at 24 weeks (**Fig. 1H**). Strikingly, both the differences in weight and glucose levels disappeared after the LL mice were returned to a standard LD cycle (**Fig. 1G-H**).

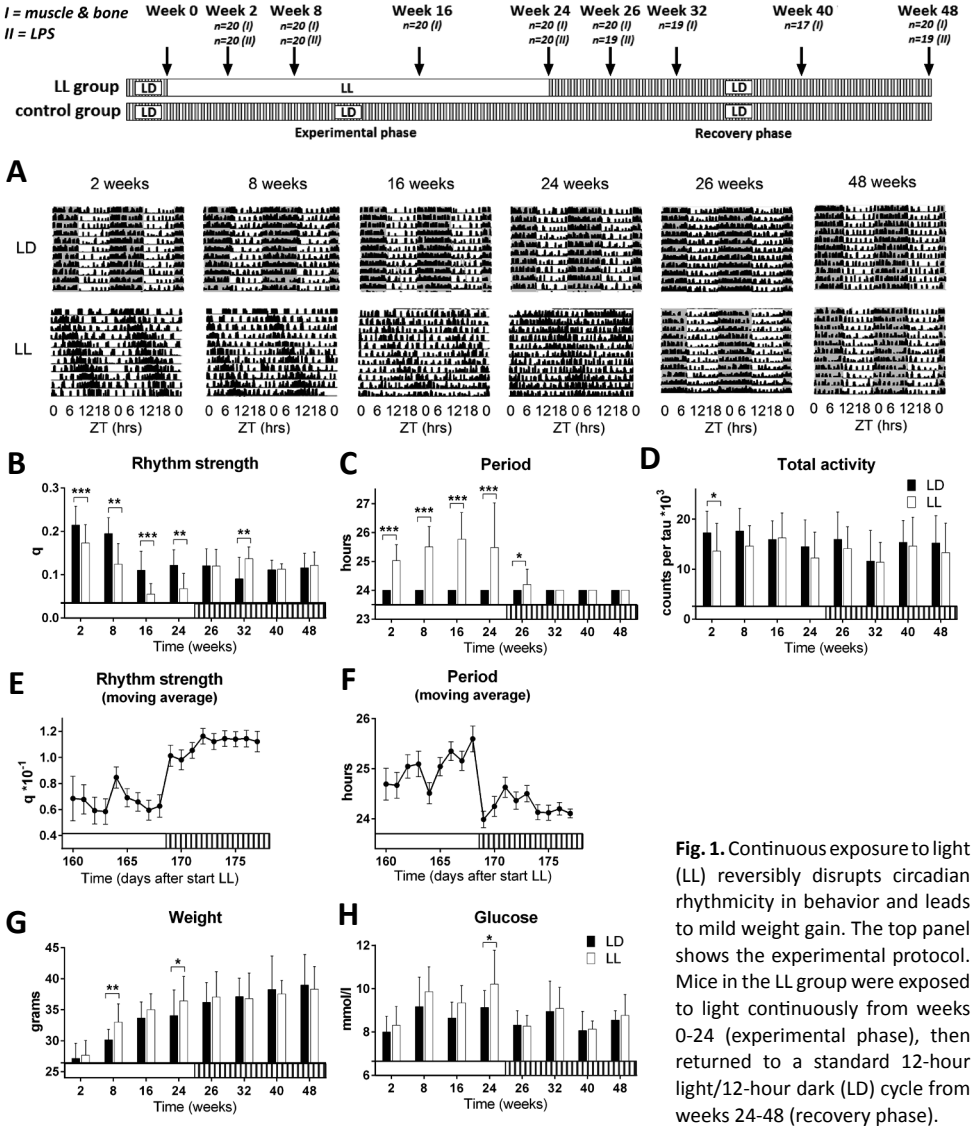

Fig. 1. Continuous exposure to light (LL) reversibly disrupts circadian rhythmicity in behavior and leads to mild weight gain. The top panel shows the experimental protocol. Mice in the LL group were exposed to light continuously from weeks 0-24 (experimental phase), then returned to a standard 12-hour light/12-hour dark (LD) cycle from weeks 24-48 (recovery phase). Mice in the control group were maintained under the standard LD cycle for the entire 48 weeks. At the indicated time points, mice were sacrificed for muscle and bone experiments or for LPS experiments. Mice used for the *in vivo* recordings are not included in the figure. (**A**) Examples of actograms recorded in LL and control (LD) mice at the indicated time points. Each horizontal row represents behavioral activity measured using a passive infrared motion detector on a double-plotted 24-hr day. Gray background represents the dark period, and white background represents the light period. (**B-D**) Rhythm strength, rhythm period, and total activity of mice in the LL and control groups at the indicated times (mean ± SD; *n* = 8-22 mice per group). (**E-F**) Five-day moving averages of rhythm strength and period in behavior in the final days of LL (or control) and in the first days after returning to an LD cycle (mean ± SEM; *n* = 22 per group). (**G-H**) Body weight and unfasted glucose levels in the LL and control groups at the indicated times (mean ± SD; *n* = 8-10 per group). The data were analyzed using a two-way ANOVA followed by post-hoc LSD. $*P < 0.05$, $**P < 0.01$, $***P < 0.001$.

Continuous light exposure attenuates neuronal rhythms in the central clock

At t = 0 (i.e., baseline), the MUA recordings revealed high-amplitude rhythms, with higher levels of electrical activity during the subjective day than during the subjective night (**Fig. 2A**). When exposed to continuous light, this amplitude decreased initially to 63% of the baseline amplitude (**Fig. 2A-B**); at 8 and 24 weeks, the amplitude was reduced further to 34% and 30% of baseline, respectively. The strength of the behavioral rhythm was strongly correlated with MUA amplitude (R^2 = 0.754, P < 0.001, Pearson correlation), and fluctuations in the strength of the SCN rhythm within individual animals occurred in parallel with fluctuations in the strength of the animal's behavioral activity rhythm. These changes in the SCN's rhythm amplitude recovered rapidly upon shifting back to a standard light-dark cycle; importantly, this recovery was mediated primarily by a reduction in the SCN's firing rate in the dark period. Proper positioning of the microelectrode in the SCN was confirmed histologically (**Fig. 2C**, **Suppl. Fig. 1**).

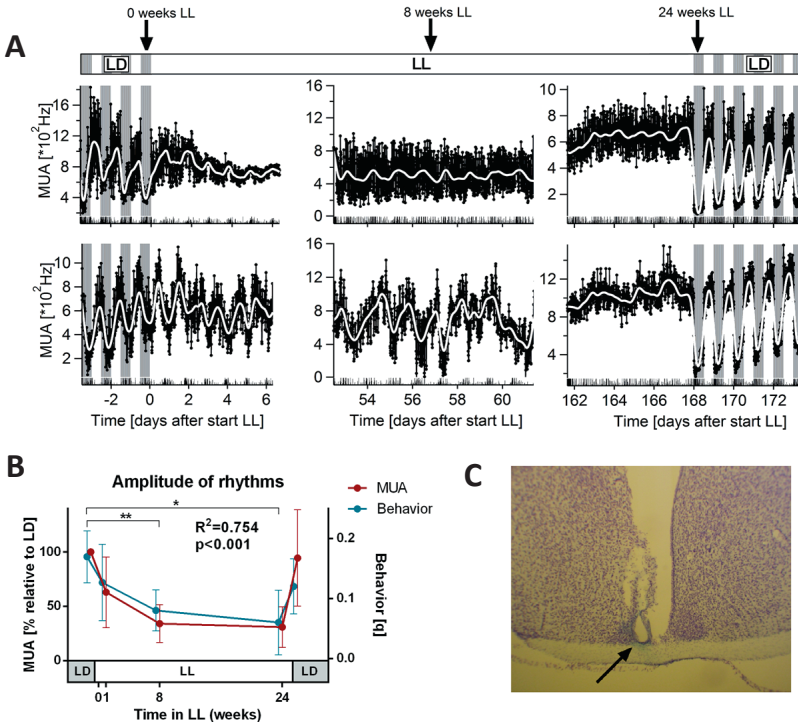

Fig. 2. Continuous exposure to light attenuates rhythmic neuronal activity in the central clock. *In vivo* recording electrodes were implanted in the SCN, and multiunit activity (MUA) was recorded in freely moving mice. (**A**) Examples of neuronal MUA rhythms recorded in the SCN of two LL mice at the times indicated. Note the more severe loss of rhythmicity in the mouse in the upper row. Gray bars indicate darkness. Behavioral activity is depicted as vertical upticks at the bottom of each graph. (**B**) Summary of the amplitude of the neuronal rhythm relative to the amplitude at baseline (red) and the strength of the behavioral rhythm of the same mice (blue). (**C**) Example of SCN histology with cresyl violet staining. The arrow indicates the location of the electrode. The third ventricle separates the two SCN nuclei that are embedded in the optic chiasm. Pearson correlation and repeated measures ANOVA, followed by post-hoc LSD; *P < 0.05, **P < 0.01.

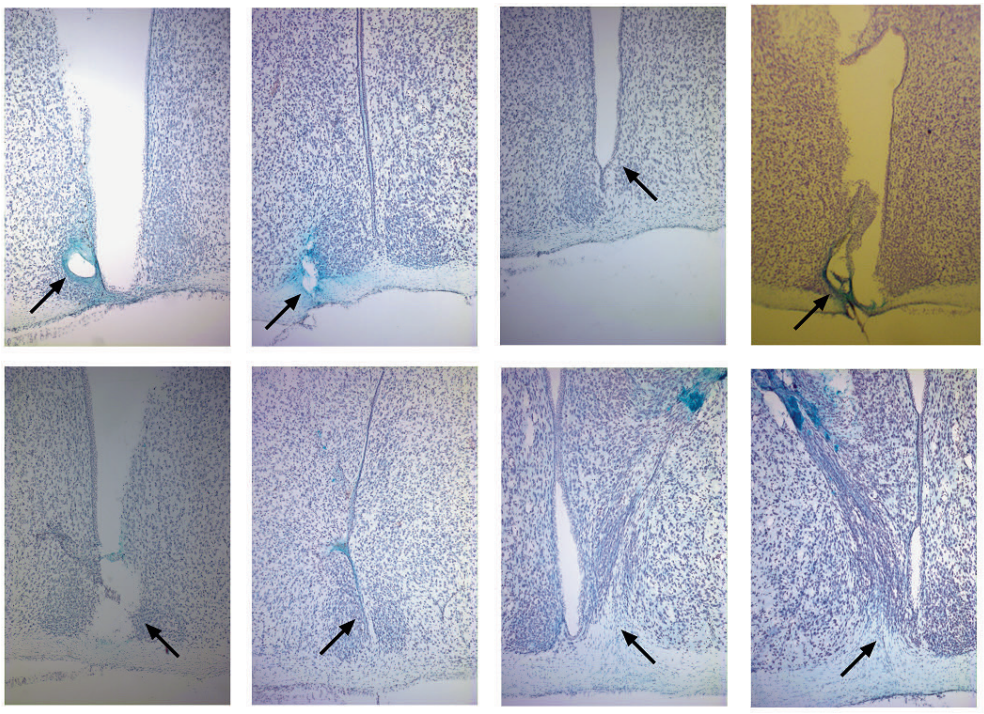

Suppl. Fig. 1: Additional histological examples showing proper placement of the electrode tip in the SCN. In each image, the arrow indicates the location of the electrode tip. The samples were stained with cresyl violet and treated with ferrocyanide, which causes a blue color reaction with the iron deposited from the electrode tip. The third ventricle separates the left and right SCN, which are embedded in the optic chiasm.

Skeletal muscle function declines in animals exposed to continuous light

Performance in all three functional muscle tests declined over time in both groups of mice. During the experimental phase, the mice in the LL group performed significantly worse in grip strength and grid hanging duration at every time point compared to the mice in the control group; performance in the wire hanging test was also worse in the LL mice, with significantly different values measured at 8 weeks (**Fig. 3A-C**). The difference in skeletal muscle function between the two groups disappeared in the recovery phase. Additional analyses in which the results were corrected for body weight and behavioral activity yielded similar results.

Both groups of mice exhibited increased fatigue-related behavior (e.g., distance walked, behavioral intensity, and time spent rearing) and anxiety-related behavior (e.g., time spent in a corner) after completing the tests as analyzed by video analysis; however, these measures did not differ significantly between the LL and control groups (**Suppl. Fig. 2**). These observations suggest that the effect of continuous light exposure cannot be attributed to a difference in motivation or anxiety.

We found no difference between the two groups with respect to absolute CK levels, the pre-test/post-test CK ratio, or the change in CK levels, indicating that LL exposure did not induce muscle damage. Although the relative amount of fibrosis in the quadriceps muscle was significantly higher in LL mice compared to control mice at 24 weeks (percentage of collagen 5 ± 1% *vs.* 4 ± 1%, respectively), this difference was too small to account for the observed differences in muscle function. We found no significant difference in the mRNA levels of macrophage (*Lgals3*, *CD68*), fibrosis (*Col1α*), regeneration (*MyoG*), mitochondrial biogenesis (*PGC1α*), or fiber type (*Myh7*, *Myh2*, and *Myh4*, which are expressed in type 1 slow fibers, type 2A fibers, and fast type 2B fibers, respectively) markers in quadriceps muscles at 8 and 24 weeks.

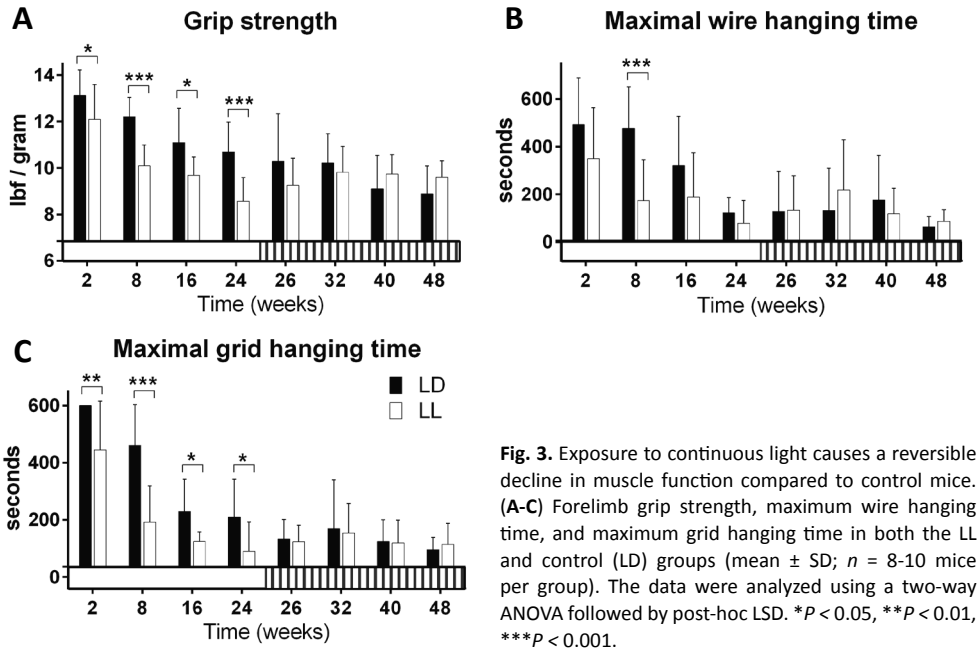

Fig. 3. Exposure to continuous light causes a reversible decline in muscle function compared to control mice. (**A-C**) Forelimb grip strength, maximum wire hanging time, and maximum grid hanging time in both the LL and control (LD) groups (mean ± SD; *n* = 8-10 mice per group). The data were analyzed using a two-way ANOVA followed by post-hoc LSD. **P* < 0.05, ***P* < 0.01, ****P* < 0.001.

Exposure to continuous light induces features characteristic of early osteoporosis

After 8 weeks in the experimental phase, both groups of mice had normal bone maturation and reached their peak relative bone volume density (BV/TV) at 20 weeks of age (**Fig. 4A, Suppl. Fig. 3A-I**). After 8 weeks of LL exposure, the metaphysis and diaphysis of the femurs had a thicker cortex compared to controls (**Suppl. Fig. 3G-I**). Over the subsequent weeks, the volume, thickness, number, and separation of the trabeculae, the structural model index (SMI), and BV/TV began to differ between the two groups (**Suppl. Fig. 3A-E**). At the end of the 24-week experimental phase, the trabeculae of the mice in the LL group were 34%

smaller in volume and 10% thinner (**Fig. 4B-C, Suppl. Fig. 3A-B**). The mice in the LL group also had 28% fewer trabeculae, which were separated more (by 16%). The trabeculae in this group were also more rod-like in shape compared to the control group. Together, these findings are characteristic of the early stages of osteoporosis.

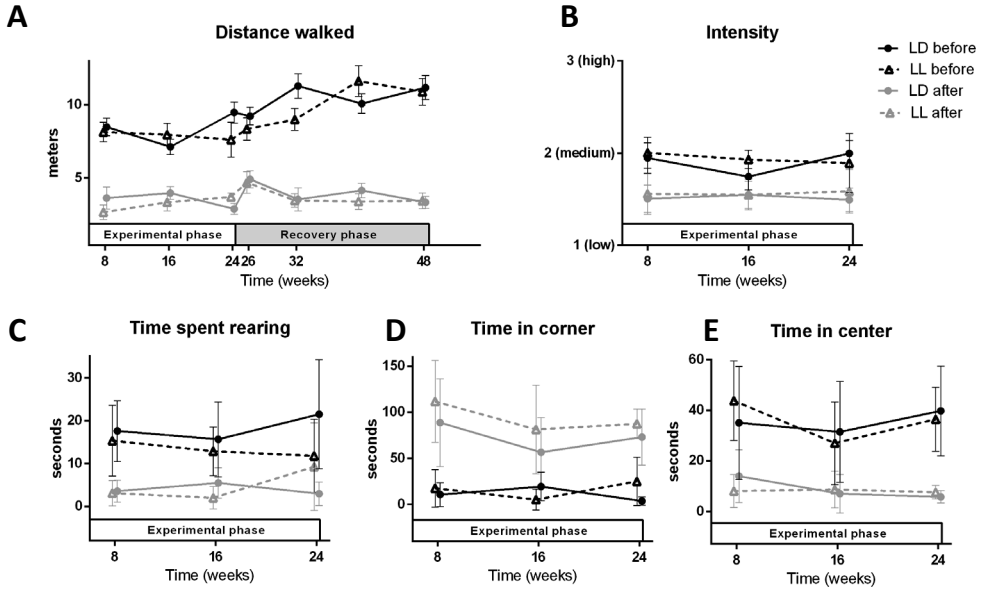

Suppl. Fig. 2: Continuous exposure to light does not affect fatigue or anxiety-related behavior measured before and after functional muscle tests. Distance walked, intensity of behavioral activity, time spent rearing, time spent in the corner, and time spent in the center of the cage were measured directly prior to (black symbols) and after (gray symbols) functional muscle tests were performed (mean ± SEM; *n* = 8-10 mice per group). All parameters were analyzed in 1-second bins from 3-minute video recordings of each mouse; the observer was blinded with respect to the group and time point. Behavioral intensity was scored subjectively as low (1), medium (2), or high (3). Generalized linear models revealed no significant differences between the groups.

In the LL group, cortical bone thickness in the metaphysis was increased by 5%; however, LL exposure had no effect on cortical volume in the metaphysis or any cortical parameters in the diaphysis (**Fig. 4B-C, Suppl. Fig. 3F-I**). Remarkably, bone structure no longer differed between LL-exposed mice and controls after returning the mice to a standard LD cycle (**Suppl. Fig. 3A-I**). Similar results were obtained when we repeated our analyses after controlling for body weight and behavioral activity levels. Lastly, consistent with age-related osteoporosis, the serum levels of calcium, phosphate, and creatinine did not differ significantly between the LL and control groups (**Suppl. Fig. 3J-L**).

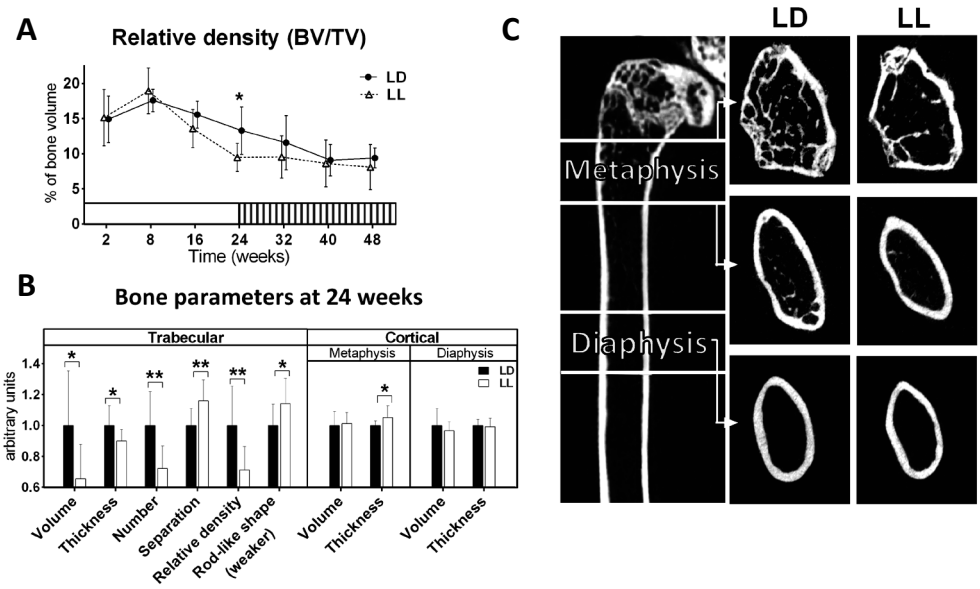

Fig. 4. Continuous exposure to light induces clinical features that are characteristic of early osteoporosis. (**A**) Relative trabecular density (BV/TV, measured as the ratio of bone volume to total volume) was measured in the LL and control groups at the indicated time points (mean ± SD; *n* = 8-9 mice per group). (**B**) Trabecular and cortical bone parameters measured at the end of the experimental phase (i.e., after 24 weeks) in LL and control mice (mean ± SD; *n* = 8-9 per group). All six trabecular bone parameters were significantly worse in the LL group. (**C**) Examples of cross-sectional microCT views of the proximal and distal metaphysis and diaphysis in LL and control mice at 24 weeks. The data were analyzed using a two-way ANOVA followed by post-hoc LSD. **P* < 0.05, ***P* < 0.01.

Exposure to continuous light alters the immune system

The total white blood cell (WBC) count was relatively unchanged throughout the experimental phase and did not differ significantly between groups (**Fig. 5A**). In contrast, both hemoglobin levels and hematocrit values were lower in the LL mice, particularly after 8 weeks of LL exposure (**Fig. 5B-C**). Also at 8 weeks, the relative number of neutrophils was nearly twice as high in the LL group, and the LL mice had fewer lymphocytes (**Fig. 5D-E**). The fraction of monocytes was higher in the mice in the LL group, particularly at 16 weeks (**Fig. 5F**). In the recovery phase, the level of monocytes returned to control levels; however, the hemoglobin and hematocrit values did not return fully to control levels. With respect to the absolute number of leucocyte subtypes, we also measured significantly more neutrophils and significantly fewer lymphocytes in the LL group at 8 weeks; in contrast, absolute number of monocytes did not differ significantly between the two groups.

After 2 weeks into the experimental phase, the mice in the LL group had lower plasma levels of IL-1β and IL-10, and they had higher plasma levels of TNF-α compared to controls (**Fig. 5G**).

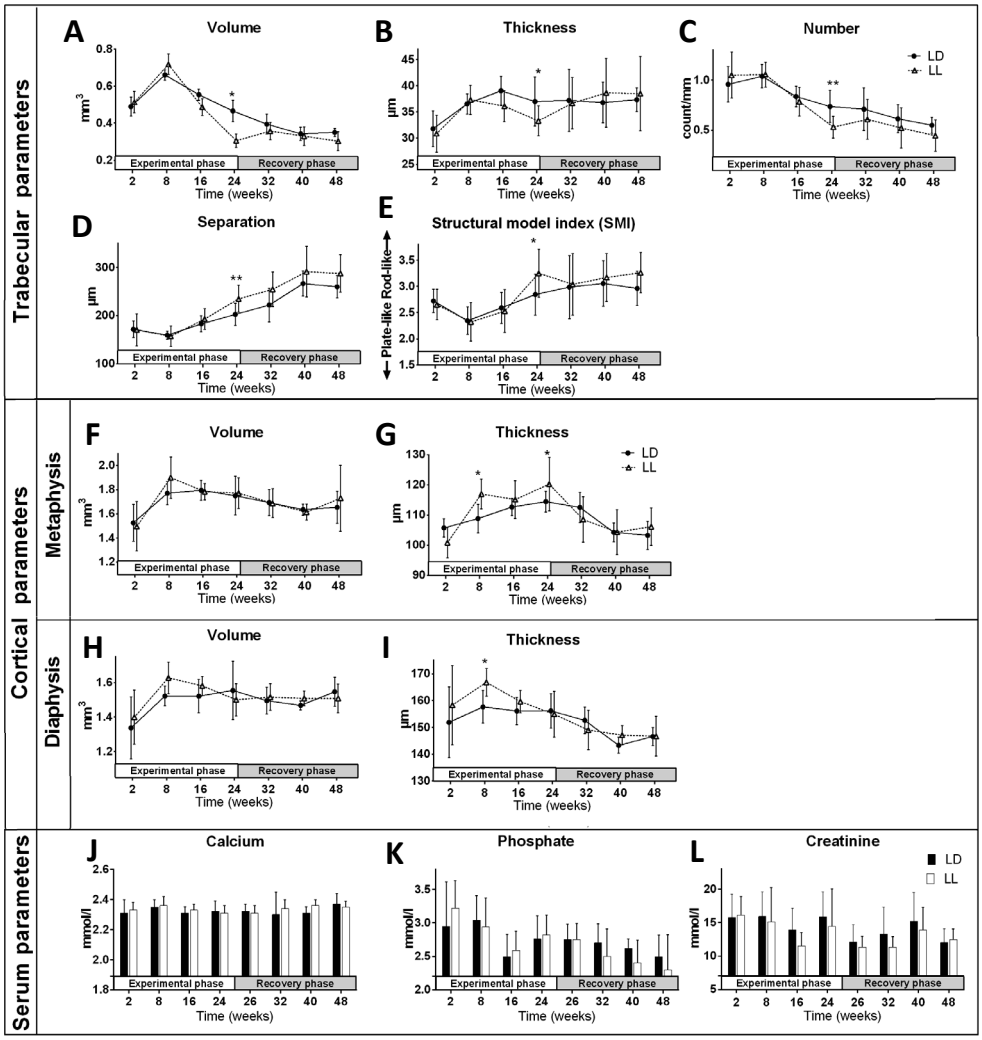

Suppl. Fig. 3: Continuous exposure to light induces changes in several bone-related characteristics. (**A-E**) Trabecular bone parameters, (**F-I**) cortical bone parameters, and (**J-L**) serum levels were measured in both LL and control (LD) mice at the indicated time points (mean ± SEM; *n* = 8-9 mice per group). The data were analyzed by two-way ANOVA followed by post-hoc LSD. **P* < 0.05, ***P* < 0.01.

Total cytokine secretion measured as the area under the curve (AUC) also differed for IL-1β and TNF-α (**Fig. 5G, Table 1**). After 8 weeks, LPS-induced secretion of the pro-inflammatory cytokines IL-1β, IL-6, and TNF-α was higher in the LL group, whereas secretion of the anti-inflammatory cytokine IL-10 was lower in the LL group. At 24 weeks, LPS-induced cytokine secretion no longer differed between the two groups. Taken together, these data suggest that LL exposure induces a transient pro-inflammatory state.

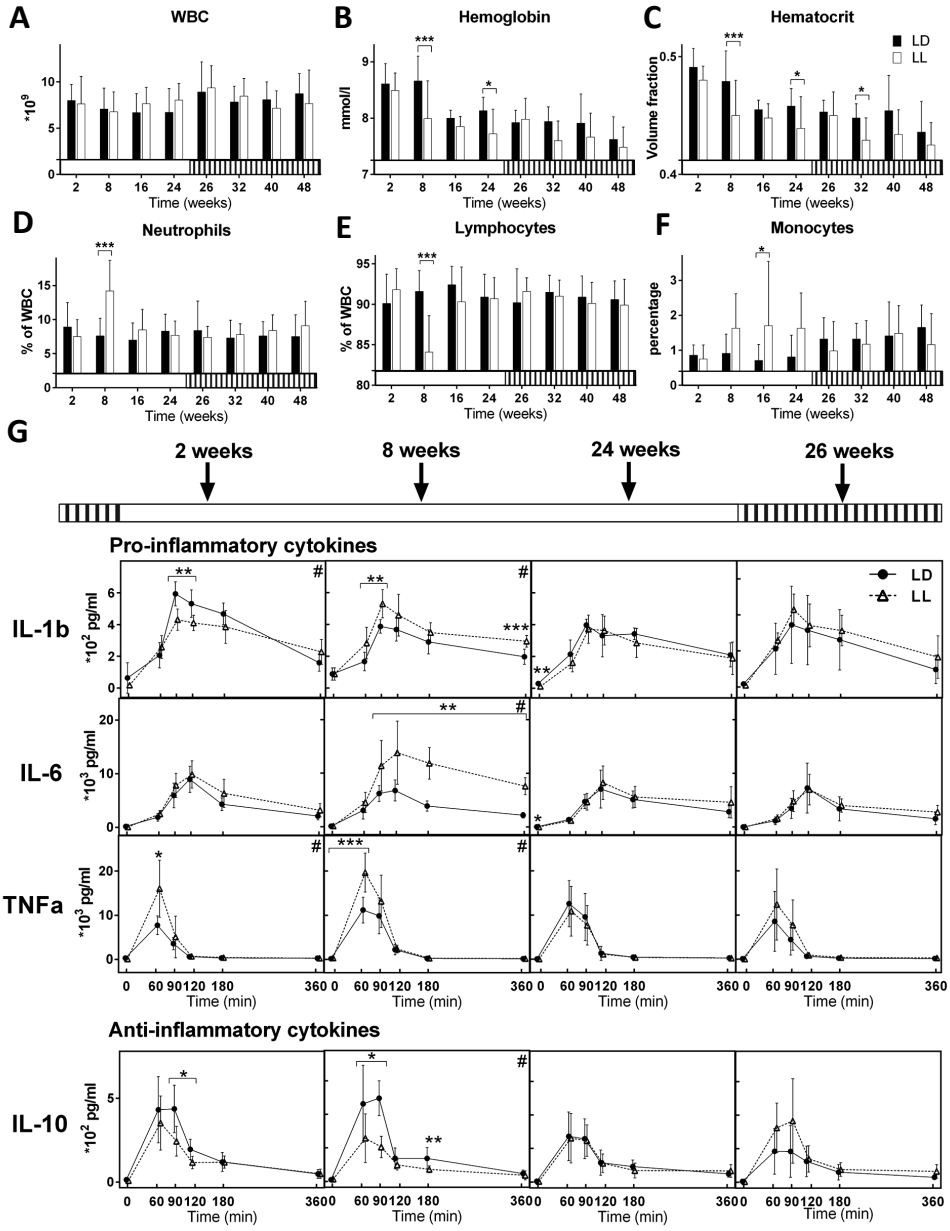

Fig. 5. Continuous exposure to light reversibly alters the homeostatic and responsive states of the immune system. (**A-F**) The indicated values were measured in LL and control mice at the indicated times. WBC, white blood cell count (mean ± SD; *n* = 8-10 mice per group). (**G**) Plasma levels of IL-1β, IL-6, TNF-α, and IL-10 were measured prior to (time 0) and 60, 90, 120, 180, and 360 minutes after an injection of low-dose LPS at the indicated experimental time points (mean ± SD; *n* = 5-12 per group). The data were analyzed using a two-way (**A-F**) or repeated-measures (**G**) ANOVA, followed by post-hoc LSD. **P* < 0.05, ***P* < 0.01, ****P* < 0.001. # in the top-right corner in panel G indicates that the area under the curve differed significantly between the two groups.

Table 1: Altered total cytokine production in response to LPS challenge in continuous light.

	2 wks		8 wks		24 wks		26 wks	
	LD	LL	LD	LL	LD	LL	LD	LL
Pro-inflammatory cytokines								
IL-1β ($x10^4$)	6.7 ± 0.9	5.0 ± 1.0**	4.7 ± 1.0	6.2 ± 1.6**	4.8 ± 0.7	4.4 ± 1.0	3.4 ± 2.6	5.0 ± 1.1
IL-6 ($x10^5$)	8.0 ± 2.3	8.5 ± 2.8	7.5 ± 1.8	13.8 ± 5.6**	6.4 ± 2.2	7.3 ± 2.3	4.7 ± 3.6	6.5 ± 2.3
TNF-α ($x10^5$)	4.7 ± 1.7	9.2 ± 4.1*	9.1 ± 3.5	14.1 ± 3.7**	9.5 ± 4.4	7.9 ± 4.1.0	4.5 ± 4.4	8.5 ± 5.6
Anti-inflammatory cytokine								
IL-10 ($x10^4$)	4.4 ± 1.4	5.8 ± 9.2	4.6 ± 1.8	2.5 ± 0.7**	2.9 ± 1.2	2.6 ± 1.2.0	1.7 ± 1.5	3.4 ± 1.7

The area under the curve (AUC) of each cytokine is shown in pg/ml/min. Data are represented as mean ± SD (*n* = 5-12 per group). Two-way ANOVA, followed by post-hoc LSD. Difference between groups at $*P < 0.05$, $**P < 0.01$.

Discussion

Exposing *C57BL/6J* mice to continuous light for 24 weeks had significant effects on the *in vivo* activity of neurons in the SCN. In addition, continuous light caused a significant decrease in skeletal muscle function and caused microstructural bone changes characteristic of the early stages of osteoporosis. Finally, mice exposed to continuous light displayed transient changes in the immune system, including a pro-inflammatory state that resolved after prolonged exposure to light. Importantly, nearly all of the physiological changes induced by long-term exposure to continuous light were reversed upon re-exposing the mice to a light-dark cycle. Taken together, these results suggest that removing cyclic environmental cues causes a reversible state of physiological vulnerability.

Exposure to continuous light decreases the strength of circadian rhythms

Retinal photoreceptors receive light and project light-encoded information to the SCN via melanopsin-containing retinal ganglion cells and chemical photoreceptors.[25,26] Continuous exposure to light causes desynchronization of SCN neurons,[22] and in peripheral bodily tissues.[27] The long-term effects of LL—as well as the system's capacity to restore rhythmicity after returning to a standard light-dark cycle—had not been studied previously and are highly relevant, given that circadian rhythms can be disrupted for extended periods, for example in shift workers or elderly persons. We confirm that short-term exposure to LL decreases neuronal amplitude[20] and demonstrate that long-term LL exposure further attenuates rhythmicity by approximately two-thirds throughout the 24-weeks of exposure. The strength of the SCN's rhythm of a given animal corresponded temporally with the strength of that animal's behavioral activity rhythm, suggesting that fluctuations in rhythm strength have a direct impact on overt behavioral rhythms.

Continuous light exposure disrupts skeletal muscle function

All mice had a decline in muscle function over time; this progressive decline in muscle function is likely due to the effects of aging.[28] The mice in the LL group had less grip strength than age-matched control mice, indicating that LL reduces muscle strength in addition to age. The mice in the LL group also had reduced physical endurance, reflected by decreased performance on the hanging tests, which require the mouse to maintain sustained force against gravity. Mice use all four limbs for hanging on a grid; in contrast, hanging on a wire is more complex and requires the coordination of several muscle groups, as well as dexterity and axial muscle strength. Even after two weeks in continuous light, the mice in the LL group showed a significant deficit, and this deficit remained throughout the experimental phase. Importantly, this decreased muscle function was independent of body weight or behavioral activity.

A video analysis of mouse behavior prior to and after functional testing revealed that the two groups of mice were fatigued to a similar extent by the testing regime. They displayed similar levels of anxiety-related behavior, suggesting that the LL-induced decline in muscle function was not due to differences in motivation. We currently have no evidence to suggest that the decreased muscle function in the LL group was due to structural differences in muscle fibrosis, muscle damage (e.g., CK levels), macrophage levels in the muscle, muscle fiber type, or differences in mitochondrial function or muscle regeneration. Previous studies have linked circadian rhythm with muscle function by examining mice with mutations in their clock genes; specifically, these mice develop structural muscle changes[1,29,30] and diminished muscle function.[1,31] However, because clock gene mutants may have impaired muscle function due to a direct effect of the clock gene mutation on the cell cycle,[32] these models do not necessarily simulate disruptions in environmental rhythmicity. Our data therefore provide first evidence, that robust external circadian rhythms support muscle function.

Continuous exposure to light induces clinical features reminiscent of early osteoporosis

Short-term (i.e., up to 8 weeks) exposure to continuous light had no effect on bone microstructure.[33] Indeed, the maturation of bone in both animal groups was similar to bone maturation in humans.[33,34] Long-term exposure to LL had a negative effect on the microstructure of cancellous (i.e., trabecular) bone; after 24 weeks, the mice in the LL group had fewer trabeculae. The remaining trabeculae were more rod-like in shape, thinner, less voluminous, and more separated, thereby resulting in decreased BV/TV compared to control mice. These changes in trabecular bone are particularly striking, as C57BL/6 mice have a relatively low BV/TV compared to other mouse strains.[33] The progressive loss of trabecular bone is believed to play the most important role in the decline in bone strength associated with age-related osteoporosis.[35] The increased thickness of cortical bone in mice exposed to continuous light may also be an accelerated effect of aging, as cortical bone mass increases

with age due to periosteal bone formation[35]; alternatively, it may represent a compensatory mechanism designed to maintain overall bone strength. Given its relatively large surface area, trabecular bone undergoes considerable turnover and remodeling; thus, osteoporotic changes are usually observed in trabecular bone first. Therefore, we feel that the changes in trabecular bone in mice exposed to continuous light are characteristic of early osteoporosis.

Of note, the levels of both calcium and phosphate were unaffected in the mice in the LL group, consistent with age-related osteoporosis in humans.[2] Moreover, general kidney function, which was assessed by measuring creatinine levels, was also unaffected by continuous light exposure.

In human studies, female shift workers have an increased risk of bone fractures[12] and decreased bone mineral density.[11] These observational studies cannot be used to determine causality, thus our results indicate for the first time that disrupted environmental rhythms are a causal factor in the decline in bone microstructure.

Circadian disruption and the immune system

Two weeks of LL exposure mildly affected LPS-induced cytokine secretion. Eight weeks of LL exposure induced a higher numbers of neutrophils, pro-inflammatory cells in the innate immune system; thus, LL appears to induce a heightened pro-inflammatory state. Consistent with this notion, the mice in the LL group had higher LPS-induced secretion of the pro-inflammatory cytokines IL-1β, IL-6, and TNF-α, coupled with decreased secretion of the anti-inflammatory cytokine IL-10. These differences were no longer observed after 24 weeks of LL exposure, suggesting that the effect of LL on the immune system is transient and/or that compensatory mechanisms may have been activated. Identifying such compensatory mechanisms would provide valuable information.

Previous studies have linked disruptions in environmental rhythms with impaired immune function. For example, shift workers have an increased risk of cancer[9] and metabolic syndrome,[36] both of which are related to immune system dysfunction.[37] Shift workers do not have altered baseline cytokine levels[38] and their immune response to challenges has not been investigated. Previous animal studies have suggested that circadian disruption is a causal factor in altered immune system function. For example, mice subjected to a chronic (i.e., 4-week) jet lag protocol have an enhanced response to LPS challenges[4] and intestinal irritant–induced colitis is more aggressive in mice that are chronically phase-shifted.[39] Moreover, exposing rats to continuous light increases mortality following LPS-induced sepsis.[40] In our experiments, we used a low, non-lethal dose of LPS; therefore, we were able to quantify the effects of an immune stimulus that more closely resembles the inflammatory response in human sepsis.[41]

Recovery of health vs. stability of health upon returning to a normal environmental cycle
After returning to a standard light-dark cycle (i.e., the recovery phase), the mice in the LL group no longer had impaired muscle performance or deficits in trabecular bone microstructure. It is difficult to assess whether restoring the light-dark cycle leads to a bona fide recovery of health, as bone microstructure and muscle function naturally decline with age. Nevertheless, in the recovery phase, many health parameters either stabilized or improved slightly, and none of the parameters measured continued to decline while muscle function and bone microstructure have the potential to decline to much lower levels, as observed in very old mice or models of severe disease.[33,43]

In the SCN, neuronal rhythmicity recovered instantaneously after returning the mice to a standard light-dark cycle. Importantly, this rapid recovery led to a large amplitude rhythm that was properly phased. The trough upon the first exposure to darkness was particularly large, suggesting that this sudden, first absence of light input acts as a "phase-resetting" stimulus for the majority of SCN neurons. Our results are consistent with a previous report in which the SCN's rhythm recovered almost immediately following a short bout of continuous light exposure.[43] Because neuronal activity is the first step in generating the output signal, and because this activity drives the release of both neurotransmitters and humoral signals, restoring the SCN's output signal will have immediate consequences for all peripheral systems that receive either direct or indirect input from the SCN.

Clinical relevance
Exposing animals to continuous light is an important model for intensive care settings and nursing homes, in which lighting can fluctuate so little throughout the 24-hour period that patients usually fail to entrain to these cycles.[44-46] For example, rhythms in behavior, body temperature, corticosteroid levels, heart rate, and melatonin levels are often disrupted—or even abolished—in intensive care patients.[47-50] Ironically, exposure to a robust environmental cycle may be particularly relevant to severely ill patients, as these patients could benefit considerably from a robust immune response. Studies have shown that preterm infants in neonatal intensive care units have improved sleep patterns and gain weight faster when exposed to a robust light-dark cycle.[51-54] In addition, nursing home residents have improved sleep and higher levels of physical activity.[55]

As 18% of elderly adults have decreased muscle strength,[56] 6 - 21% have osteoporosis,[57] and immune system dysregulation can aggravate age-related pathologies,[58] large segments of the elderly population are at increased risk for frailty. A frail state in the elderly could be explained by a decline in their circadian system, since the changes in rhythm amplitude in the SCN in the LL group are reminiscent of rhythm changes that occur in the clock of aged individuals.[59] Therefore, the LL-induced decline in mice may represent the contribution of an "aged" clock to the age-related decline in health.

Conclusions

Here, we provide insight into the long-term effects of disrupted environmental rhythmicity on several major health parameters, and we provide evidence that the majority of these effects are reversible. We conclude that complex temporal relationships involved in daily fluctuations in muscle function, bone microstructure and immune function are disrupted by exposure to continuous light, and this disruption underlies the observed changes in health. These results create new opportunities for prevention and treatment programs, particularly for frail individuals, such as intensive care patients, nursing home residents and the elderly. Our results are also highly relevant to large segments of the population, as three-quarters of the world's population is routinely exposed to artificial light during the night.[6] We propose that long-term prospective studies should be performed to examine the health effects of increasing diurnal light levels in such settings. For example, in addition to increasing light levels during the day,[60] light exposure during the night can be reduced easily without compromising patient safety.[61] The long-term effects of a robust light-dark cycle on muscle function, bone microstructure, and the immune system are currently unknown in humans. Our study provides compelling evidence that the detrimental effects of chronic continuous light exposure warrant further investigation.

Methods

Study design

Adult male *C57BL/6JOlaHSD* mice (Harlan, Horst, the Netherlands) were group-housed in Macrolon cages (35×36 cm) in sound-tempered chambers; food and water were available *ad libitum*. Mice were housed under constant ambient temperature (22°C). At the age of 12 weeks, the mice were randomly assigned to various groups. The mice in the "LL group" were exposed continuously to a light source (Naturalite light bulb; 76 $\mu W/cm^2$ = 105 lux) for 24 weeks ("experimental phase"); during this phase, mice in the "LD (control) group" were exposed to a 12-hour light/12-hour dark cycle. After the 24-week experimental phase, the mice were exposed to the standard light-dark cycle for an additional 24 weeks ("recovery phase"). Body weight was measured at least every two weeks.

The mice in the LL and control groups were further divided into three subgroups. One group of mice was used for muscle and bone experiments; these animals were dissected at 2, 8, 16, 24, 26, 32, 40, and 48 weeks relative to the start of the experimental phase. A second group of mice was subjected to a lipopolysaccharide (LPS) challenge at 2, 8, 24, and 26 weeks. In the third group of mice, *in vivo* SCN neuronal activity was recorded longitudinally (n = 9). All experiments were performed at circadian time 0 (CT0), which corresponds to the start of the animal's active phase. A total of 271 mice were used for these experiments.

Behavioral data

Two weeks prior to beginning the experiments, the mice were transferred to individual cages equipped with passive infrared (PIR) motion detectors (Hygrosens Instruments, Löffingen, Germany) placed underneath the lid of the cage. Because the location of the nest can influence total activity levels and rhythm strength, we ensured that the nest was located at the end of the cage furthest from the PIR sensor by rotating the cage when necessary. During the experiments, the nest was in the optimal location for all but three mice. The PIR detectors were connected to a ClockLab data collection system (Actimetrics, Wilmette, IL). Data recorded on the first day of the experiments were excluded from the analysis. The strength and period of the behavioral rhythm were determined by F periodogram analysis of PIR recordings in 10-minute bins.[62] Rhythm strength was defined as the difference between the 95% confidence limit and the peak in the periodogram. The total number of counts per period was averaged for the individual mice and then adjusted to a 24-hour period (e.g., a value of 1000 counts during 25 hours was adjusted to 960 counts per 24 hour period).

Muscle function tests

Four days before dissection, muscle function tests were performed at CT0 in accordance with the TREAT-NMD Network protocol (http://www.treat-nmd.eu/resources/research-resources/dmd-sops.[42] Forelimb grip strength was measured using a grip strength device (Columbus Instruments, Columbus, OH) in five trials consisting of three attempts, with a two-minute interval between each trial. The three highest values were then averaged. During the wire hanging test, the mice had three attempts to hang for 10 minutes from a rigid metal wire. For the grid hanging test, the mice were placed on an inverted grid in order to assess maximum grid hanging time; the mice had three attempts to hang for 10 minutes. The mice were allowed to rest for three minutes between each attempt, with 45 minutes between each test. Before the muscle function tests, unfasted glucose levels were measured from a drop of blood obtained via a small tail cut; glucose was measured using glucose strips (Accu-Chek Aviva, Reeuwijk, Netherlands). Blood was also collected in 0.3 ml Microvette CB300 tubes before and after the functional testing; the blood was centrifuged at 4°C for 5 minutes at 13,000 rpm. Plasma creatine kinase (CK) levels were measured using Reflotron CK test strips in a Reflotron Plus machine (Roche Diagnostics Ltd., Burgess Hill, UK) within three hours of collection. The mice were also video-recorded using an AXIS 221 Network Camera for three minutes in a new cage before and directly after the muscle function tests. Both cages contained the scent of other mice to stimulate exploratory behavior. Video analyses were performed by a researcher who was blinded with respect to the experimental conditions and time point. Total walking distance was determined manually using Mousetracker software (SuperEasy GmbH & Co, www.supereasy.net). The intensity of behavioral activity was scored per second as “1” (least intense), “2” (moderately

intense), or "3" (most intense). The time spent in the corner, in the center, and rearing were also measured.

Dissection and tissue processing

Mice were euthanized under deep anesthesia with 50 mg/kg ketamine and 0.5 mg/kg dexdomitor, and blood was collected by retro-orbital bleeding. Blood was collected in Microtainer tubes containing K_2EDTA (Becton Dickinson B.V., Breda, the Netherlands) for whole blood analysis and in uncoated Eppendorf tubes for serum analysis. The quadriceps muscles were dissected, snap-frozen in 2-methylbutane (Sigma-Aldrich, Zwijndrecht, the Netherlands), then stored in liquid nitrogen. Femurs were fixed in 4% paraformaldehyde for 48 hours and then stored in 70% ethanol at 4°C.

Serum bone marker analysis

Serum levels of calcium, phosphate, and creatinine were measured with a Modular P800 chemical analyzer (Roche Diagnostics, Indianapolis, IN), using a colorimetric (calcium and phosphate) or enzymatic (creatinine) method. The analytical variability of each test is <2.5%.

Muscle histology

Sections (8-µm thick) were cut using a Shandon cryotome (Thermo Fisher Scientific, Waltham, MA) and affixed to Superfrost Plus slides (Thermo Fisher Scientific). The remaining muscle tissue was collected in tubes containing MagNa Lyser Green Beads (Roche Diagnostics) and used to isolate RNA for qPCR experiments. The sections were stained with goat anti-Collagen type 1 primary antibody (dilution 1:100; 1310-01 Southern Biotech, Birmingham, AL) followed by donkey anti-goat Alexa594 secondary antibody (dilution 1:1000; Invitrogen Life Technologies Europe B.V., Bleiswijk, the Netherlands); the nuclei were counterstained with DAPI. The sections were examined using a model DM5500 B fluorescence microscope (Leica Microsystems B.V., Son, the Netherlands) at 10x magnification, and images covering the entire muscle were captured using a DC350 FX digital camera. The percentage of fibrotic tissue was quantified using ImageJ software (National Institutes of Health, Bethesda, MD; downloaded from http://rsb.info.nih.gov/ij/).

qPCR

The quadriceps muscle was obtained at 8-week and 24-week time points as described above. Total RNA was isolated from the samples using the phenol-chloroform extraction method (Tripure RNA Isolation Reagent, Roche) and quantified by NanoDrop. First-strand cDNA was synthesized from 1 µg of total RNA using the Superscript First-strand Synthesis Kit (Thermo Fischer Scientific). Real-time PCR assays were performed using specific primer sets (sequences provided upon request) with SYBR Green in a CFX Real-Time PCR system

(Bio-Rad, Veenendaal, the Netherlands). mRNA levels were normalized to the housekeeping gene *Gaphd* and are expressed as arbitrary units.

MicroCT measurements

Femurs stored in 70% ethanol were scanned using a Skyscan 1076 X-ray microtomograph (Skyscan, Aartselaar, Belgium). Scan parameters included a 40-kV, 250-µA X-ray source with a 1-mm Al filter (to reduce beam hardening artifacts) and a step size of 0.8° covering a trajectory of 180°. Images were reconstructed at 9.12-µm isotropic voxel size using NRecon software (V1.6.2.0, Skyscan) with ring artifact correction set to 5 and beam hardening correction set to 20%. Femurs were reoriented with the mid-diaphysis parallel to the *z*-axis, and 15-mm long regions were selected in the diaphysis and distal metaphysis (0.3 mm under the epiphysis). Reconstructed grayscale images were segmented using an automated algorithm with local thresholds[63] in order to distinguish calcified tissue from non-calcified tissue. The trabeculae and cortex were identified using the software program PrStackBot-New (Orthopedic Research Laboratory, Erasmus Medical Center, Rotterdam, the Netherlands). Bone morphometric parameters were determined in the distal metaphysis and the diaphysis using 3D-Calculator (Skyscan).

Whole blood analysis

Whole blood was analyzed within six hours of collection using an automated Sysmex XE-2100 blood cell counter (Sysmex Cooperation, Kobe, Japan). Total and differential white blood cell (WBC) counts were determined using flow cytometry with forward-scatter, side-scatter, and lateral fluorescent light.[64] Hemoglobin and hematocrit values were measured using the sodium lauryl sulfate-hemoglobin and RBC pulse-height detection methods, respectively. The results were confirmed by performing a light-microscopy examination of hematoxylin and eosin–stained blood smears from ten mice.

LPS challenge and cytokine analysis

At CT0, mice were injected intravenously with 50 µg/kg LPS (*E. Coli* O111:B4, purified by ion-exchange chromatography, catalog number L3024, Sigma, St. Louis, MO). Tail blood was collected in 0.3 ml Microvette CB300 tubes directly prior to LPS injection and 60, 90, 120, 180, and 360 minutes after injection; after collection, the blood samples were centrifuged at 1,000 rpm for 15 minutes. The supernatant was collected and centrifuged at 10,000 rpm for 10 minutes; this supernatant was stored at -80°C. Plasma cytokine levels were measured using the Bio-Plex Protein Array System and a mouse cytokine panel (Bio-Rad). IL-1β, IL-6, IL-10, and TNF-α concentrations were measured using the Bio-Plex Manager software program. The AUC was calculated for each cytokine at each time point.

In vivo SCN electrophysiology

At an age of 12 to 15 weeks , a separate group of mice was anesthetized with 100 mg/kg ketamine, 20 mg/kg xylazine, and 1 mg/kg atropine, and a tripolar stainless steel electrode (PlasticsOne, Roanoke, VA) was implanted using a stereotaxic setup (Stoelting Europe, Dublin, Ireland). Two polyimide-insulated electrodes were aimed at the SCN (0.61 mm lateral of Bregma, 5.38 mm below the dura, at a 5° angle) for differential neuronal recordings, and a reference electrode was placed in the cortex. Following a one-week recovery period, the electrodes were connected to a custom-made recording system via a flexible cable with a counterbalanced swivel system that enabled the animals to move freely. After the signal was amplified and filtered (0.5-5 kHz), action potentials were detected with window discriminators and stored in 10-sec epochs (Circa V1.9, custom-made software). Multiunit activity (MUA) was recorded for 3 days in a standard LD cycle and for the first 7 days in LL. Mice were then recorded at 8 and 24 weeks in LL, and upon returning to a regular LD cycle. The mice in the control group were not subjected to continuous light. Behavioral activity was recorded simultaneously using a PIR sensor. Mice were disconnected from the recording system to minimize traction on the electrode. Rhythm strength of behavioral activity was measured using F periodogram analysis. The MUA signal was smoothed using a penalized least-squared algorithm.[65] Amplitude (peak height minus the average height of the adjacent troughs) was measured from the smoothed signal. After recording, the animals were sacrificed, and a small electric current was passed through the electrode to deposit iron at the site of the electrode tip. The brains were collected and fixed in 4% formaldehyde containing ferrocyanide to stain the iron deposited from the electrode tip. The brains were stained with cresyl violet, and placement of the electrode tip in the SCN was confirmed histologically.

Statistics

All statistical analyses were performed using SPSS 20.0 for windows (IBM Corp., Armonk, NY) or the R 3.0.1 statistics package (Foundation for Statistical Computing, Vienna, Austria) using the VGAM package.[66,67] Normality of data was tested using the Shapiro-Wilk test and Q-Q plots. Two-way ANOVAs were performed and, in case of significance ($P < 0.05$), the Fisher's Least Significant Difference (LSD) procedure was used to compare the LL and control groups at each time point. Analyses were performed separately for the exposure and recovery phases of the experiment. Repeated-measures ANOVA with post-hoc LSD were performed to analyze the longitudinal data. Because the wire hanging and grid hanging trials had a cut-off value of 600 seconds, the effect of LL was examined using Tobit regression with accounting for censored effects. Dummy variables were used to compare the LL and control groups at each time point. In mice that were exposed to LL for 24 weeks and then returned to a standard 12-hour light/12-hour dark cycle, a five-day moving average was

calculated for period and rhythm strength. Pearson's correlation coefficient was calculated to determine the correlation between the rhythm strength of behavior and MUA measured in each mouse. Generalized linear mixed models using a compound symmetry covariance structure were constructed for analyzing the video data. Optimal distributions and link functions were determined using the Akaike Information Criterion.

Study approval
All experiments were approved by the Leiden University Medical Center's Ethics Committee for Animal Experimentation.

Author Contributions

E.A.L., J.H.M., J.S., A.A.R., H.H.S., B.G., and C.W.G.M.L. designed the experiments. E.A.L., M.v.P., S.R.d.K., R.P.M.S., J.G., S.L.V., M.v.d.V., and K.E.d.R. performed the experiments. E.A.L. and J.H.M. wrote the paper, and C.P.C., A.A.R., M.v.P., S.R.d.K., S.L.V., H.H.S., B.G., J.S., K.E.d.R., and C.W.G.M.L. provided comments on the final manuscript.

Acknowledgements

We thank Heleen Post-van Engelendorp Gastelaars for excellent overall practical assistance. Furthermore, we thank Marcel de Winter, Leonie Forsman, and Thomas Vogels for their help with experiments; Peter Stouten for outstanding SCN histology; Gerard van der Zon for mRNA analyses; Arifa Ozir-Fazalalikhan and Alwin van der Ham for practical assistance with luminex experiments; the hematological laboratory (CKHL) at Leiden University Medical Center for serum measurements; and Margreet de Vries, Adri Mulders, Zeen Aref, and Simone Haberlein for assistance and advice regarding the storage of organic materials. We are grateful to Jos Rohling and Tom Deboer for technical support regarding the circadian analyses; Ralf Werring for technical advice regarding muscle histology; Jimmy Berbée, Els van Beelen, Gerard Haasnoot, Els van der Meijden, Ulysse Ateba Ngao, and Khalil Boutaga for advice regarding LPS experiments; Fred Reymer for advice regarding Sysmex analyses; Jolanda Verhagen and Bart Ballieux for help with serum measurements; and Yuri Robbers and Jeanine Houwing-Duistermaat for advice regarding statistics. **Funding:** This research was funded by the Netherlands Organization for Scientific Research grant TOPGO.L.10.035 (to J.H.M) and by the Dutch Diabetes Research Foundation grant 2013.81.1663 (to C.P.C.). **Competing Financial Interests:** The authors have declared that no conflict of interest exists.

References

1. Andrews JL, Zhang X, McCarthy JJ, et al. (2010) CLOCK and BMAL1 regulate MyoD and are necessary for maintenance of skeletal muscle phenotype and function. *Proc Natl Acad Sci U S A* 107:19090-19095.
2. Eastell R, Calvo MS, Burritt MF, et al. (1992) Abnormalities in circadian patterns of bone resorption and renal calcium conservation in type I osteoporosis. *J Clin Endocrinol Metab* 74:487-94.
3. Takarada T, Kodama A, Hotta S, et al. (2012) Clock genes influence gene expression in growth plate and endochondral ossification in mice. *J Biol Chem* 287:36081-36095.
4. Castanon-Cervantes O, Wu M, Ehlen JC, et al. (2010) Dysregulation of inflammatory responses by chronic circadian disruption. *J Immunol* 185:5796-5805.
5. Bennie J, Davies TW, Duffy JP, Inger R, Gaston KJ (2014) Contrasting trends in light pollution across Europe based on satellite observed night time lights. *Sci Rep* 21:3789.
6. Cinzano P, Falchi PF, Elvidge CD (2001) The first World Atlas of the artificial night sky brightness. *Mon Not R Astron Soc* 328:689–707.
7. Lee S, McCann D, Messenger JC (2007) Working time around the world. Trends in working hours, laws and policies in a global perspective. Routledge, New York, ed. 1. [first edition]
8. Alterman T, Luckhaupt SE, Dahlhamer JM, Ward BW, Calvert GM (2013) Prevalence rates of work organization characteristics among workers in the U.S.: Data from the 2010 National Health Interview Survey. *Am J Ind Med* 56:647–59.
9. Stevens RG, Brainard GC, Blask DE, Lockley SW, Motta ME (2014) Breast cancer and circadian disruption from electric lighting in the modern world. *CA Cancer J Clin* 64:207-18.
10. Pietroiusti A, Neri A, Somma G, et al. (2010) Incidence of metabolic syndrome among night-shift healthcare workers. *Occup Environ Med* 67:54-57.
11. Quevedo I, Zuniga AM (2010) Low bone mineral density in rotating-shift workers. *J Clin Densitom* 13:467-469.
12. Feskanich D, Hankinson SE, Schernhammer ES (2009) Nightshift work and fracture risk: the Nurses' Health Study. *Osteoporos Int* 20:537-542.
13. Obayashi K, Saeki K, Iwamoto J, et al. (2014) Effect of exposure to evening light on sleep initiation in the elderly: a longitudinal analysis for repeated measurements in home settings. *Chronobiol Int* 31:461-467.
14. Obayashi K, Saeki K, Iwamoto J, et al. (2013) Exposure to light at night, nocturnal urinary melatonin excretion, and obesity/dyslipidemia in the elderly: a cross-sectional analysis of the HEIJO-KYO study. *J Clin Endocrinol Metab* 98:337-344.
15. Obayashi K, Saeki K, Iwamoto J, Ikada Y, Kurumatani N (2014) Association between light exposure at night and nighttime blood pressure in the elderly independent of nocturnal urinary melatonin excretion. *Chronobiol Int* 31:779-786.
16. Aubrecht TG, Weil ZM, Nelson RJ (2014) Dim light at night interferes with the development of the short-day phenotype and impairs cell-mediated immunity in Siberian hamsters (Phodopus sungorus). *J Exp Zool A Ecol Genet Physiol* 321:450-456.
17. Bedrosian TA, Fonken LK, Walton JC, Nelson RJ (2011) Chronic exposure to dim light at night suppresses immune responses in Siberian hamsters. *Biol Lett* 7:468-471.
18. Fonken LK, Weil ZM, Nelson RJ (2013) Mice exposed to dim light at night exaggerate inflammatory responses to lipopolysaccharide. *Brain Behav Immun* 34:159-163.
19. Fonken LK, Lieberman RA, Weil ZM, Nelson RJ (2013) Dim light at night exaggerates weight gain and inflammation associated with a high-fat diet in male mice. *Endocrinology* 154:3817-3825.
20. Coomans CP, van den Berg SA, Houben T, et al. (2013) Detrimental effects of constant light exposure and high-fat diet on circadian energy metabolism and insulin sensitivity. *FASEB J* 27:1721-1732.
21. Qian J, Yeh B, Rakshit K, Colwell CS, Matveyenko AV (2015) Circadian disruption and diet-induced obesity synergize to promote development of β-cell failure and diabetes in male rats. Endocrinology 156:4426-36.
22. Ohta H, Yamazaki S, McMahon DG (2005) Constant light desynchronizes mammalian clock neurons. *Nat Neurosci* 8:267-269.
23. Nováková M, Polidarová L, Sládek M, Sumová A (2011) Restricted feeding regime affects clock gene expression profiles in the suprachiasmatic nucleus of rats exposed to constant light. *Neuroscience* 197:65-71.
24. VanderLeest HT, Houben T, Michel S (2007) Seasonal encoding by the circadian pacemaker of the SCN. *Curr Biol* 17:468-73.
25. Foster RG, Hankins MW, Peirson SN (2007) Light, photoreceptors, and circadian clocks. *Methods Mol Biol* 362:3-28.

26. van Diepen HC, Ramkisoensing A, Peirson SN, Foster RG, Meijer JH (2013) Irradiance encoding in the suprachiasmatic nuclei by rod and cone photoreceptors. *FASEB J* 27:4204-12.
27. Polidarová L, Sládek M, Soták M, Pácha J, Sumová A (2011), Hepatic, duodenal, and colonic circadian clocks differ in their persistence under conditions of constant light and in their entrainment by restricted feeding. *Chronobiol Int* 28:204-215.
28. Karakelides H, Nair KS (2005) Sarcopenia of aging and its metabolic impact. *Curr Top Dev Biol* 68:123-148.
29. Kondratov RV, Kondratova AA, Gorbacheva VY, Vykhovanets OV, Antoch MP (2006) Early aging and age-related pathologies in mice deficient in BMAL1, the core component of the circadian clock. *Genes Dev* 20:1868-1873.
30. Pastore S, Hood DA (2013) Endurance training ameliorates the metabolic and performance characteristics of circadian Clock mutant mice. *J Appl Physiol (1985)* 114:1076-1084.
31. Bae K, Lee K, Seo Y, Lee H, Kim D, Choi I (2006) Differential effects of two period genes on the physiology and proteomic profiles of mouse anterior tibialis muscles. *Mol Cells* 22:275-284.
32. Fu L, Lee CC (2003) The circadian clock: pacemaker and tumour suppressor. *Nat Rev Cancer* 3:350-361.
33. Halloran BP, Ferguson VL, Simske SJ, et al. (2002) Changes in bone structure and mass with advancing age in the male C57BL/6J mouse. *J Bone Miner Res* 17:1044-1050.
34. Jilka RL (2013) The relevance of mouse models for investigating age-related bone loss in humans. *J Gerontol A Biol Sci Med Sci* 68:1209-1217.
35. Brandi ML (2009) Microarchitecture, the key to bone quality. *Rheumatology* 48:iv3-iv8.
36. Wang F, Zhang L, Zhang Y, et al. (2014) 0147 Meta-analysis on night shift work and risk of metabolic syndrome. *Occup Environ Med* 71 Suppl 1:A78.
37. Seijkens T, Kusters P, Chatzigeorgiou A, Chavakis T, Lutgens E (2014) Immune cell crosstalk in obesity: a key role for costimulation? *Diabetes* 63:3982-3991.
38. Copertaro A, Bracci M, Gesuita R, et al. (2011) Influence of shift-work on selected immune variables in nurses. *Ind Health* 49:597-604.
39. Preuss F, Tang Y, Laposky AD, et al. (2008) Adverse effects of chronic circadian desynchronization in animals in a "challenging" environment. *Am J Physiol Regul Integr Comp Physiol* 295:R2034-R2040.
40. Carlson DE, Chiu WC (2008) The absence of circadian cues during recovery from sepsis modifies pituitary-adrenocortical function and impairs survival. *Shock* 29:127-132.
41. Deitch E (1998) Animal models of sepsis and shock: a review and lessons learned. *Shock* 9:1–11.
42. van Putten M, Hulsker M, Young C, et al. (2013) Low dystrophin levels increase survival and improve muscle pathology and function in dystrophin/utrophin double-knockout mice. *FASEB J* 27:2484-95.
43. Chen R, Seo DO, Bell E, von Gall C, Lee C (2008) Strong resetting of the mammalian clock by constant light followed by constant darkness. *J Neurosci* 28:11839-11847.
44. Verceles AC, Silhan L, Terrin M, Netzer G, Shanholtz C, Scharf EM (2012) Circadian rhythm disruption in severe sepsis: the effect of ambient light on urinary 6-sulfatoxymelatonin secretion. *Intensive Care Med* 38:804-45. Riemersma-van der Lek RF, Swaab DF, Twisk J, Hol EM, Hoogendijk WJ, van Someren EJ (2008) Effect of bright light and melatonin on cognitive and noncognitive function in elderly residents of group care facilities: a randomized controlled trial. *JAMA* 299:2642-2655.
46. Bullough J, Rea MS, Stevens RG (1996) Light and magnetic fields in a neonatal intensive care unit. *Bioelectromagnetics* 17:396-405.
47. Freedman NS, Gazendam J, Levan L, Pack AI, Schwab RJ (2001) Abnormal sleep/wake cycles and the effect of environmental noise on sleep disruption in the intensive care unit. *Am J Respir Crit Care Med* 163:451-457.
48. Olofsson K, Alling C, Lundberg C, Malmros C (2004) Abolished circadian rhythm of melatonin secretion in sedated and artificially ventilated intensive care patients. *Acta Anaesthesiol Scand* 48:679-684.
49. Gehlbach BK, Chapotot F, Leproult R, et al. (2012) Temporal disorganization of circadian rhythmicity and sleep-wake regulation in mechanically ventilated patients receiving continuous intravenous sedation. *Sleep* 35:1105-1114.
50. Paul T, Lemmer B (2007) Disturbance of circadian rhythms in analgosedated intensive care unit patients with and without craniocerebral injury. *Chronobiol Int* 24:45-61.
51. Miller CL,White R, Whitman TL, O'Callaghan MF, Maxwell SE (1995) The effects of cycled versus noncycled lighting on growth and development in preterm infants. *Infant Behavior & Development* 18:87-95.
52. Morag I, Ohlsson A (2013) Cycled light in the intensive care unit for preterm and low birth weight infants. *Cochrane Database Syst Rev* 8:CD006982.

53. Watanabe S, Akiyama S, Hanita T, et al. (2013) Designing artificial environments for preterm infants based on circadian studies on pregnant uterus. *Front Endocrinol* 4: 1-11.
54. Vásquez-Ruiz S, Maya-Barrios JA, Torres-Narvaez P, et al. (2014) A light/dark cycle in the NICU accelerates body weight gain and shortens time to discharge in preterm infants. *Early Hum Develop.* 90: 535-540.
55. Alessi CA, Martin JL, Webber AP, Cynthia Kim E, Harker JO, Josephson KR (2005) Randomized, controlled trial of a nonpharmacological intervention to improve abnormal sleep/wake patterns in nursing home residents. *J Am Geriatr Soc* 53:803-10.
56. Looker AC, Wang CY (2015) Prevalence of reduced muscle strength in older U.S. adults: United States, 2011-2012. *NCHS Data Brief* 179:1-8.
57. Kanis JA (2000) An update on the diagnosis of osteoporosis. *Curr Rheumatol Rep* 2:62-6.
58. Michaud M, Balardy L, Moulis G, et al. (2013) Proinflammatory cytokines, aging, and age-related diseases. *J Am Med Dir Assoc* 14:877-882.
59. Nakamura TJ, Nakamura W, Yamazaki S, et al. (2011) Age-related decline in circadian output. *J Neurosci* 31:10201–10205.
60. White RD (2004), Lighting design in the neonatal intensive care unit: practical applications of scientific principles. *Clin Perinatol* 31:323-30, viii.
61. Walsh-Sukys M, Reitenbach A, Hudson-Barr D, DePompei P (2001) Reducing light and sound in the neonatal intensive care unit: an evaluation of patient safety, staff satisfaction and costs. *J Perinatol* 21:230-5.
62. Dörrscheidt GL, Beck L (1975) Advanced methods for evaluating characteristic parameters (alpha, tau, rho) of circadian rhythms. *J Math Biol* 2:107-121.
63. Waarsing JH, Day JS, Weinans H (2004) An improved segmentation method for *in vivo* microCT imaging. *J Bone Miner Res* 19:1640-1650.
64. Walters J, Garrity P (2000) - Laboratory hematology - Carden Jennings. Performance evaluation of the Sysmex XE-2100 hematology analyser.
65. Eilers PH (2003) A perfect smoother. *Anal Chem* 75:3631–3636.
66. R Core Team, R: A language and environment for statistical computing. R Foundation for Statistical Computing, Vienna, Austria. ISBN 3-900051-07-0, URL http://www.R-project.org/ (2012).
67. Yee TW, Wild CJ (1996) Vector Generalized Additive Models. *Journal of Royal Statistical Society* 58:481-493.